NovaSAR and SSTL S1-4: SAR and EO Data Fusion

Rebecca Couchman-Crook, Avyaya Kolhatkar, Tobie Carman
Defence Science and Technology Laboratory
DSTL Portsdown West, Portsdown Hill Road, Fareham, Hampshire, PO17 6AD
novasar-s1@dstl.gov.uk

Jess Park, James Lambert, Claire Morris
Defence Science and Technology Laboratory
RAF Wyton, Huntingdon, Cambridgeshire PE28 2EA

ABSTRACT

The NovaSAR and SSTL S1-4 satellites were launched into a 580 km sun-synchronous orbit on 16th September 2018[1]. NovaSAR is an S-band Synthetic Aperture Radar (SAR) platform, and SSTL S1-4 hosts a multi-spectral (RGB, NIR) and panchromatic electro-optical (EO) high-resolution payload[1]. As the satellites are adjacent in orbit, with NovaSAR leading SSTL S1-4 by ~15 minutes, this provides an opportunity to demonstrate the benefits of using SAR and EO data together. The key demonstration principles are: to show the complementary nature of near-contemporaneous SAR and EO data, tipping and cueing opportunities of a tandem sensor, and to demonstrate the superiority of one technology for a specific application. The ability to undertake enhanced vessel detection using machine learning algorithms, to use bathymetry with EO and SAR imagery to get a more complete picture, and to detect oil spills in SAR imagery have been demonstrated. This proves the capability of the technologies, and their strengths as joint and separate data sources, helping to inform future mission concepts.

1 SATELLITES – NOVASAR AND SSTL S1-4

Launched on the Polar Satellite Launch Vehicle (PSLV) into a Sun-synchronous orbit (SSO) from India, NovaSAR and SSTL S1-4 are currently adjacent, 15 minutes apart, in their position 580 km above the Earth.[1]

1.1 NovaSAR

NovaSAR is a SAR platform, designed as a small low-cost satellite, able to support an S-band SAR payload.[3] The mission has a 7 year lifetime, of which, for the first year or so, it has been in tandem with the SSTL S1-4.[3]

NovaSAR carries an Automatic Identification System (AIS) receiver that can be used to detect signals from ships, with information on their location and identity. This could be used to validate ship detections within the SAR maritime surveillance images.[3]

It is capable of imaging with single and dual polarisation in StripMap and Maritime modes, and these in addition to tri-polar in ScanSAR. Stripmap mode has the best resolution of 6 m, with ScanSAR achieving 20 m resolution. The Maritime mode is a 400 km-wide swath, designed for the observation of larger expanses of water, and subsequent vessel detection.[3]

1.2 SSTL S1-4

SSTL S1-4 is an electro-optical platform, designed to observe land for disaster monitoring. It uses the same design as the UK-DMC satellites launched previous to it.[4]

The imager is capable of <1 m GSD in panchromatic mode and <4 m GSD in multispectral mode (Red: 600-670nm, Green: 510-590nm, Blue: 440-510nm, NIR: 760-910nm). It has the capability of area, strip and stereo imaging modes, with a swath of around 21 km.[2]

2 NEAR-CONTEMPORANEOUS SAR AND EO DATA

With SSTL S1-4 ~15 minutes behind NovaSAR, this provides an excellent opportunity to demonstrate the complementary nature of having SAR and EO data alongside one another, capturing the same scenes ~15 minutes apart. This section covers a few potential examples of uses that would exploit this capability.

2.1 Camouflage

It is possible to see how targets look in both visible bands and SAR, and with the closeness of the acquisitions, it allows for validation of potential target identifications in SAR imagery, such as ships. This can

be acted on as more accurate information than just the one data type on its own.

2.2 Bathymetry

Using multi-spectral EO for bathymetry has been done previously, and there is merit in examining how SAR data complements these bathymetric estimates. The acquisition of images at near-enough the same time for bathymetric purposes allows a useful comparison to be drawn.

2.3 Machine Learning

Building a set of near-contemporaneous images allows for a training set of images to be made to facilitate machine learning of targets. This lends itself to creating a better set of training data to aid vessel detection, and in theory would allow for training on one set to be tested on another, to see if this gave better recognition of targets.

2.4 Vessel Detection and Ship Wakes

Ship wakes are visible at multiple wavelengths, and they show particularly well in S-band SAR, seen in multiple NovaSAR acquisitions. They can show movement on the water, even when an accompanying vessel is not clear. SSTL S1-4 imagery taken not long after the NovaSAR acquisition can help to show vessels in more detail at a finer resolution than SAR.

Given the all-weather day/night capability of SAR, ship detection from SAR imagery is well established for maritime surveillance applications. In benign weather conditions with calm sea states the radar backscatter from the sea surface is typically low when compared to the radar cross section of a large vessel, making vessel detection achievable with a simple constant false alarm rate (CFAR) detector. However, maritime surveillance modes are typically wide swath and reasonably low resolution for maximum coverage. This mode may not be available for the entire duration, so instead high sea states and ScanSAR can prove the same principles. This means that small vessels, or vessels with low radar cross section, may be difficult to detect. SSTL S1-4 EO imagery is collected at a higher resolution and thus more likely to detect small vessels or vessels of low radar cross section. Furthermore, the spectral response of the vessel may help aid identification.

2.5 Topography Correction of SAR using EO Stereo

Features of SAR images that make interpretation more complicated are foreshortening and layover. They arise due to variations in local topography particularly in mountainous regions. For example, two points on a mountain slope facing the SAR platform have a shorter slant range distance between them than two points in a valley. This leads to the compression of backscattered information in the range direction from the mountain slope faces in the ground-projected image and is known as foreshortening. If the slope face is particularly steep, there may be ambiguous returns whereby a point on the slope face has the same slant range distance as a point on the valley floor and in this case the return from the slope face is laid over on the return from the valley floor in the ground-projected image. Foreshortening effects are correctable in post-processing and geo-coding with a suitable digital terrain model.

SSTL S1-4 has the capability of collecting an along track (single pass) high resolution stereo scene pair of a target location. Standard photogrammetric procedures can be used to orientate the images and extract a digital surface model for the target location. This surface model could then be used to correct the foreshortening effects seen in the SAR image collected for the same area.

2.6 Confirm Target Authenticity

Each sensor provides validation for the other if a target looks suspicious. Additionally, with the AIS sensor on board NovaSAR, vessel identities can be shown in more detail, and this can give greater assurance. This can also be aided by ground-truth data.

2.7 Landing Strip Availability and Quality

In the SAR and EO images, the appearance of the landing strips can be compared, to see how features in the runway appear in both. The availability of the airstrip can also be determined and checked, and any subsequent movement of planes and vehicles in the intervening ~15 minutes, by comparing the images.

2.8 Coherent Change Detection using EO to Fill Shadows

A SAR sensor is an active sensor, meaning that RF illumination of a target is provided by the sensor itself. Depending upon the acquisition geometry this can result is some shadowing effects within the collected image region.

With a passive EO sensor, the illumination is from the Sun, which, depending on the Sun angle, will result in either no shadow, or shadow in different places to those that exist in the SAR image. The equator crossover time

for SSTL S1-4 is 10:30, so shadows are likely to be minimal for most of the year. Therefore, the additional information from the EO sensor can be used to "fill" any shadows from the SAR image taken, and allow for greater detail to be seen. Vice versa, one can use SAR to fill in information for cloudy regions in EO data[7].

3 CUEING A TANDEM SENSOR

With NovaSAR in front of SSTL S1-4, having two images taken ~15 minutes helps to validate findings from one scene to another. While the satellites do not have a cueing feature, due to no intersatellite links, we trialled how each sensor compliments the other, to unlock new utilities using this feature of the satellites' positons in space. This demonstrates the potential a tipping and cueing system could have. This section will show some of the applications this could have if intersatellite links existed between the sensors.

3.1 Camouflage

If a target is camouflaged in one sensor, perhaps information about how it is camouflaged, could be found by cueing a following sensor to image the same scene if it was suspected there was a camouflaged object in it. The Near Infra-Red (NIR) band on-board SSTL S1-4 could potentially show if any natural camouflage was used.

3.2 Dark Vessel Detection

AIS technology is well utilised for Maritime Domain Awareness, with transceivers sending data regarding a vessel's name, type, position, heading, velocity etc. every 2 to 10 seconds. However, the system is vulnerable to both spoofing and disablement. The large swath coverage and all weather day/night operation of SAR sensors and the ability to detect ships within SAR imagery makes it a valuable source of intelligence for comparison and combination with AIS data. Anomalous vessels can be identified if they are detected in a SAR image but cannot be associated with a ship location or ship track derived from contemporaneous AIS data. Understanding the limitations of space-based AIS is key for this; it is known that it is best used in open waters.

Cueing and tasking of SSTL S1-4 behind NovaSAR, would allow for better identification of what the identity of any "dark vessel" might be, especially with the finer resolution available from the Panchromatic mode of <1 m.

3.3 Landing Strip Availability and Quality

If an airstrip was imaged in SAR, showing as a long dark straight line, any planes will also be detected, with their metallic structures showing as bright points.[6]

Using detection of them to cue SSTL S1-4, would allow for the finer resolution EO imagery to help in identifying plane type, number of planes and the quality of a landing strip.

3.4 Movement of a Target

If a target is observable in the SAR data from NovaSAR, it might be then possible to monitor its movement in the intervening 15 minutes, when SSTL S1-4 would pass overhead and be able to image the target. This application would pose some difficulties, as moving targets in SAR are displaced, and this would need correcting before comparison. From this, direction and speed of motion could be determined, therefore, this might show where a target was ultimately heading.

4 SUPERIORITY OF SAR AND EO FOR DIFFERENT APPLICATIONS

Some applications lend themselves well to a particular technology, either because of the wavelength used and its interactions with the atmosphere, or due to some things simply not being visible using that method of detection because of the materials they are made from. This section explores some of the benefits and limitations of SAR and EO imagers for these tasks.

4.1 Camouflage

Particularly in defence settings, many targets are largely metal-based or concrete buildings. These show up very clearly in SAR images. Therefore, corners and walls of camouflaged buildings and vehicles may be uncovered by using SAR, whereas they may be hidden in EO imagery.

4.2 Bathymetry

The penetration of SAR into water bodies is not extensive, perhaps a few 10s of metres, and water is often black in SAR images, especially if it has an undisturbed surface, due to the forward scatter on the smooth surface. Thus, we can struggle to tell much depth information from just a SAR image, though this

might be possible from gravity and Bragg wave structures on the sea surface.

EO imagery, taken at differing wavelengths will show different features with each wavelength due to the varying water penetration by them, especially with the addition of blue and green bands. EO has greater sensitivity at shallower depths than SAR S-band, but SAR has a greater range of depth. Together they can provide more complete bathymetric information, and separately provide depths when there's cloud cover (obscuring an EO image) or rough sea states (SAR is unable to retrieve depths in these conditions).

4.3 Hidden Objects and Forest Penetration

Canopy penetration will be greatest with S-band SAR. EO imagery cannot 'see' through the layers of leaves, but can give an indication of vegetation health, through the Normalised Differentiation Vegetation Index (NDVI).

SAR on the other hand, can show the structure of what lies underneath, with X-band showing canopy/low penetration detail, and L-band giving more details of the ground surface as it is higher penetration. Therefore, the S-band payload on-board NovaSAR can show detail down to trunk-level in a forest.

4.4 Oil Spills

SAR has been used to identify oil spills, with algorithms in place for their detection, such as in the Sentinel Applications Toolbox (SNAP) from ESA. As oil disrupts the wave pattern on the water's surface, reducing the surface roughness, it will stand out against the noisier surroundings due to a chaotic sea state. It also offers the opportunity to detect image spills through cloud and at night. This gives it an advantage over EO imagery, but MSI imagery has been used to detect this.[5]

4.5 Time and Weather Dependency

In inclement weather, particularly in cloudy conditions and moderate rainfall, SAR will have the upper-hand as it can detect through cloud, whereas an EO system would just take a white scene.

SAR also has the benefit of being able to image at night, as it is a passive technology, so it is not reliant on illumination from other sources, like electro-optical imagers. Though night-time optical imaging may be a useful avenue for some use cases.

4.6 Wavelength and Colour Detection

For colour detection. EO would have the clear advantage, as the EO payload can image in different wavelengths (Red, Green Blue and NIR). Some targets imaged may have unique spectral characteristics which will show with different combinations.

5 DEMONSTRATED UTILITIES

Using the data from NovaSAR and SSTL S1-4, we have explored some of these use cases, to see what advantages the near contemporaneous collection gives, and prove that these sensors have the capability to support these research objectives.

5.1 Scene Interpretation

The wavelength buildings and objects are imaged in, and the material they are made of, can influence whether they seemingly appear or disappear in SAR and EO images.

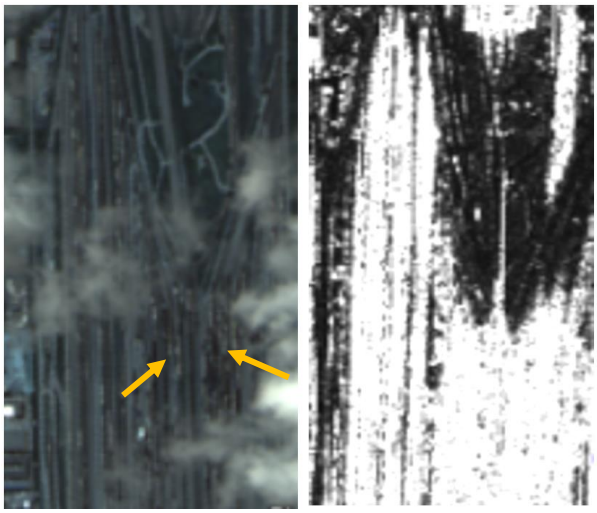

Figure 1: A view of Toronto Train Station, showing the natural RGB image from SSTL S1-4 on the left and the SAR image from NovaSAR on the right, where the detail of the train carriages is lost in the S-band wavelength when compared to the RGB image. © SSTL

This can act as a kind of camouflage in different wavelengths, additionally obscuring the outline of an

object, so only part is visible. This can make interpretation of a scene difficult.

A high presence of "bright" objects in SAR imagery can oversaturate the received signals and mask out details of the shape of an object in an area. This can be seen by a number of train carriages present in Fig. 1 that blur any details as to the number of carriages and their shape. The source of the bright objects can clearly be seen as individual train carriages in the EO image of the same scene; however, some of the image is obscured by clouds, which is not a feature in the SAR image. This shows that both bring different information about a scene that add to the interpretation of what is contained in the image.

5.2 Vessel Detection

Two automated ship detection approaches were trialled on the source data from NovaSAR. The first, a traditional method of land-masking, modelling sea surface clutter and applying a Constant False Alarm Rate (CFAR) algorithm. The second, training a RetinaNet-based Convolutional Neural Network (CNN) with S-band and C-band data to detect ships.

The CNN method used one set of training data from Sentinel-1 and Gaofen-3, which are C-band SAR sensors. This was applied to the NovaSAR testing set of imagery. It was verified that non-native training data could be used to detect ships in S-band data. Further to this, the CNN method of ship detection out-performed the CFAR method in the absence of native training data, and also with and without landmasks applied. It was also noted that the RetinaNet CNN could detect ships based on their wake alone, when the ships themselves were hard to see.

The conclusions from this work are tentatively drawn, due to a small dataset to test on, with lack of variety of sea states. Importantly however, the findings of a CNN method of detection working better than a CFAR method with no native training data, suggests that this technology could provide an integrated ship detection capability from the start of operations in something akin to the NovaSAR platform, avoiding the need of amassing training sets first.

(Additional details as to this work may be found in Carman, T. and Kolhatkar, A., 2020, *A Comparison of CFAR and CNN vessel detection methods for S-band NovaSAR images*.)

5.3 Dark Vessel Detection

Combining SAR images from NovaSAR with AIS data received from NovaSAR allows for the identification of dark vessels.

In practice, the combining of the data in congested waterways was a challenge, as it was harder to attribute signals to ship, and their AIS broadcasts may not have been received, even though they were transmitted.

In less crowded waters, images have been tagged with the corresponding AIS data, and ships without information are much more easily identified (see bottom left bright pixels with no orange label in Fig. 2).

This could be taken further by combining with knowledge of water depth (potentially utilising the bathymetry work) to provide evidence of illicit activity, i.e. something labelled as a tanker should not be in very shallow waters.

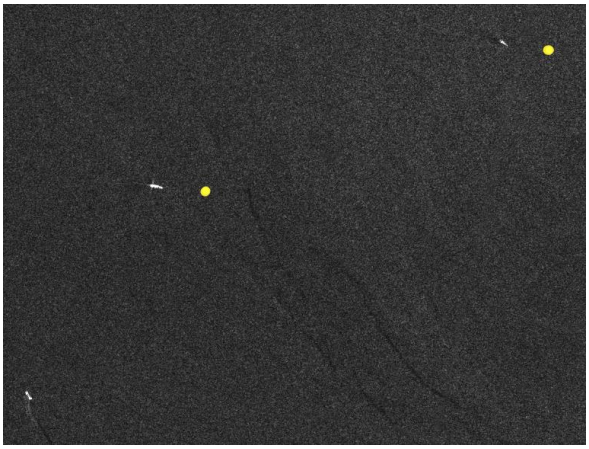

Figure 2: A NovaSAR SAR image with NovaSAR AIS data overlaid, denoted by orange dots. © SSTL

5.4 Target Movement

Using images from both NovaSAR and SSTL S1-4 we have been able to track the movement of vessels in the ~15 minute window between the two images (see Fig. 3). The speed (and distance) at which the vessel is going can be determined by using the time interval between acquisitions and the distance covered by the ship. Additionally, this technique can be used against accompanying AIS data to verify the identity and intentions of vessels.

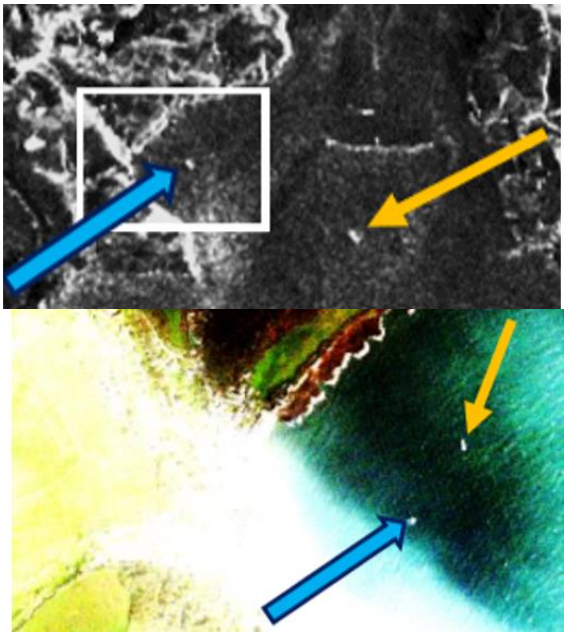

Figure 3: A view of British waters, where a boat is seen moving into the area outlined in the white box on the NovaSAR SAR image (top), in the SSTL S1-4 natural colour RGB image taken ~15 minutes later (bottom). © SSTL

5.5 Vegetation Index

By using the different bands in the multi-spectral images from SSTL 1-4, we are able to create a variety of vegetation indices. Health of the vegetation can be seen by the classic NDVI (Near-Infrared band minus Red band, divided by Near-Infrared band plus Red band). Using two other band combinations we have shown utility for classifying vegetation coverage and ground type.

The combination of Near Infra-Red, Red and Green, assigned to Red, Green, Blue respectively, can provide a similar indicator as to what is vegetation, what is water and what is bare land, (see Fig. 4).

Comparing this band combination with the NovaSAR image provided clarification as to rectangular features that were visible in SAR, but had differing levels of reflectivity. It was seen that this was due to the level of vegetation in those areas.

Another useful combination that gives indication as to the ground cover and the vegetation that is at that location is provided by the band combination Near Infra-Red, NDVI and Green, as Red, Green and Blue respectively. (see Fig. 5). In this band variation, non-vegetated land appears in magenta (commonly buildings and sand) and dark blue (commonly water). Vegetation coverage can be classified with greener areas being closed canopy, acid yellow being open canopy or shrubs, and golden yellow shows areas of grass.

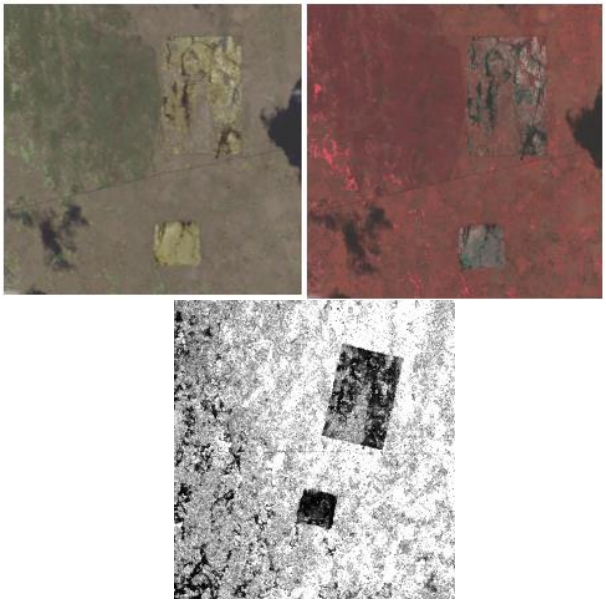

Figure 4: A view of the Everglades, US. The natural colour RGB on the left and NIR-R-G band combination on the right, both from SSTL S1-4. Below is the NovaSAR image of the same scene. © SSTL

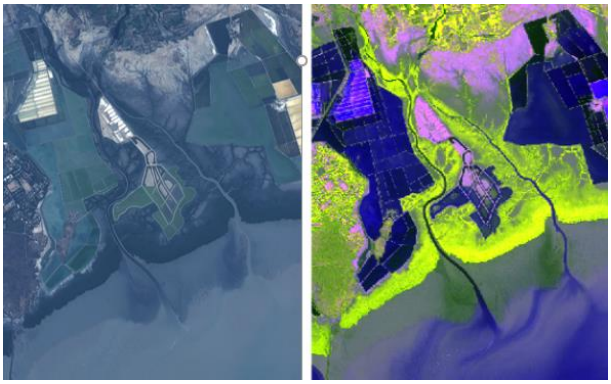

Figure 5: A view of the Bay of Bengal, India. The natural colour RGB on the left and NIR-NDVI-G band combination on the right, both from SSTL S1-4. © SSTL

5.6 Bathymetry

The bathymetry of shallow coastal areas was investigated for both SAR and EO data. There is an existing methodology for the extraction of water depth from EO imagery, which allowed for the depths to be extracted from SSTL S1-4 imagery. However, the processing of the NovaSAR imagery required a new methodology to output water depths from SAR data.

For the purposes of bathymetry, the images can be considered contemporaneous, due to the long period of any bathymetric changes. This use case explored whether SAR or EO gave more accurate estimates,

based on ground-truth data, and if when combined, the results could provide better accuracy.

5.6.1 SAR Bathymetry

SAR bathymetry data extraction requires a fully calibrated and georeferenced file, exhibiting Bragg scattering and with given swell data. Wave directions are estimated across the image by overlapping subsets of the image and 2D FFTs, to produce power spectrum estimates. These give a peak in wavenumber that are translated to a local peak wavelength for each subset.[8] The wavelengths are combined with the linear wave dispersion relation to estimate the local depth, *h*, at each point on the image. The angular frequency of the waves, *w*, is calculated by using a known value for a point of deep water in the image (from ground-truth) (see Eqn. 1).[9] The depths for each point calculated across the different sub-images will then be averaged.[10]

$$h = \frac{L}{4\pi} ln\left(\frac{2\pi g + w^2 L}{2\pi g - w^2 L}\right) \quad (1)$$

Fig. 6 gives an example of the output from this method. The systematic error from the SAR output, comparing the estimated depth with the local charted depth, is in line with other reported errors in S-band SAR bathymetry studies, at 25%.

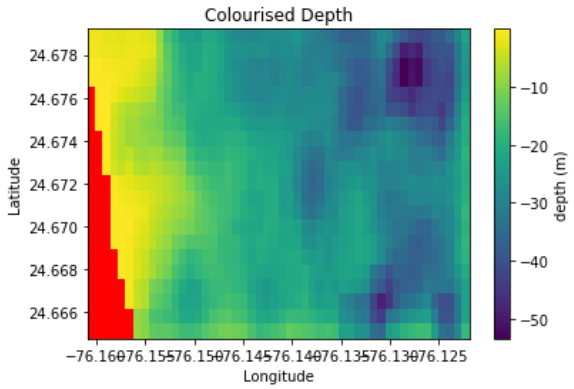

Figure 6: This graph shows the estimated depth for each point in the image subset for SAR data taken of Princess Cays, Bahamas. The red area denotes a landmask.

5.6.2 Electro-Optical Bathymetry

Electro-optical bathymetry data extraction requires measurement of the depth that different wavelengths of light detected by the sensor can penetrate to. This requires a land mask to be applied, using data from the NIR band, though clouds and boats can cause issues in this method.

The depth of each pixel is found by applying the Stumpf formula (Eqn. 2) to the green and blue bands.[11] This is applied using the Marlin Water Depth Tool in the ENVI platform (not part of the standard ENVI package).

$$z = m_1\left(\frac{\ln(L_{obs}(Band_b))}{\ln(L_{obs}(Band_g))}\right) - m_0 \quad (2)$$

With L_{obs} is the observed radiance for each band, and m_1 and m_0 are the offset and gain.

The Lyzenga algorithm can also be used, which uses the log-linear relationship of reflectance and depth, considering the total reflectance from all bands in the image.[12]

Analysis on an example EO image of Princess Cays, Bahamas, showed that the Stumpf method performed better with areas containing obstacles like reefs. The Lyzenga method produced lower errors by comparison over smooth areas. Both methods were limited to a depth of 20 m due to the penetration of the ocean by optical wavelengths.

When the bathymetric data has been extracted from the EO and SAR images, they can be compared to ground-truthing data. They can then provide alternative methods of bathymetric data retrieval, when another method is not viable. SAR may be unusable in chaotic sea states, and EO would not work in cloud covered scenes. SAR has a greater range in depth, but EO data provides greater sensitivity at shallow depths. The data could also be combined to minimize errors in values obtained from a scene, where the depth estimates overlap in the 10-20 m range.

5.8 Oil Spill Detection

Oil spills appear dark in SAR imagery, as they alter the surface texture of the water.[13] Two methods were employed to extract oil spill information from an image, these were a texture analysis GLCM method, and another was an in-built oil spill detection algorithm in the Sentinel Applications Toolbox (SNAP). The methods were used on an oil spill image of Nigeria, and trialled in HH and VV polarisations.

In the GLCM (Grey Level Co-occurrence Matrix) method, the image was speckle filtered and multi-looked to reduce noise and speckle in the image. Then, using the SNAP Toolbox inbuilt GLCM, a variety of textural analyses can be retrieved.[14] From these, the Entropy image provides the greatest contrast for picking out the oil spill from the image.

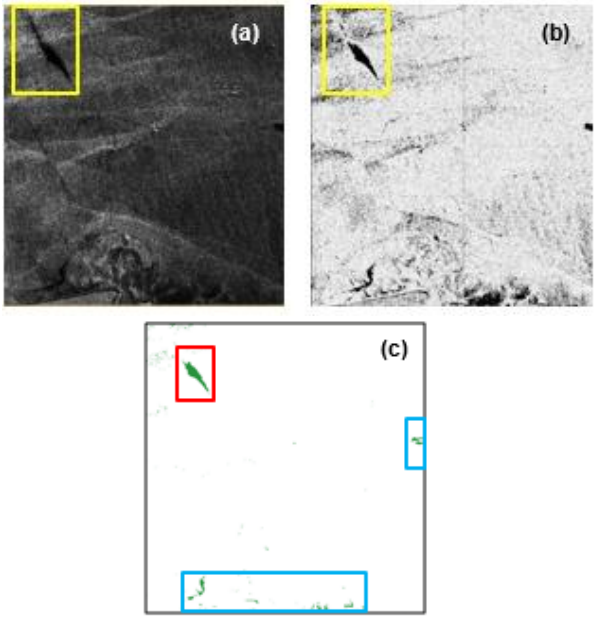

Figure 7: Images detailing an oil spill near Nigeria, in HH polarisation, with (a) the original speckle filtered and multi-looked image, (b) the GLCM entropy image, (c) the K-means cluster image with the oil spills picked out in green. © SSTL

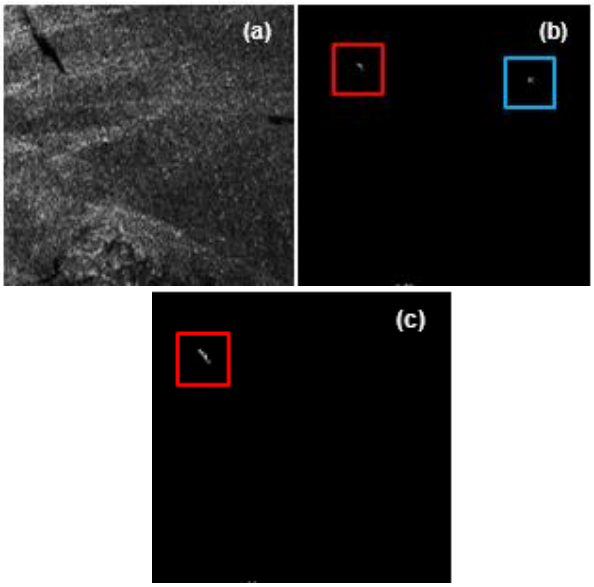

Figure 8: Images detailing an oil spill near Nigeria, in HH polarisation, with (a) the original speckle filtered image, (b) the SNAP inbuilt oil spill detection with default settings, (c) the SNAP inbuilt oil spill detection with readjusted variables. © SSTL

Then an unsupervised K-Means classification was implemented, and by colouring the clusters white, the oil spill was picked out from the background by colouring one cluster green (or any other colour). Some anomalous pixels are notable (see Fig. 7), but the application of a land mask would help to omit many of these.

The second method uses the inbuilt SNAP Oil Spill Detection tool. The scenes were landmasked, then a scene-specific threshold was used to detect points, and then a clustering algorithm was used to classify these as a spill if the area was over a certain amount. Less anomalous pixels were visible, but the extent of the oil spill is poorly defined (see Fig. 8).

A near-contemporaneous EO image of the oil spill scene was not retrieved, so comparisons for EO and SAR for oil spill detection could not be tested in this study. However, it is likely that together, the EO and SAR would show the oil spill's greatest extent when processed images were overlaid, though SAR is generally favoured for this application,

CONCLUSION

Utility has been demonstrated in a variety of areas for near contemporaneous EO and SAR imagery, combined with AIS data. This has much to recommend it as a sensor combination for future mission concepts. The benefits of particular sensors for certain applications has also been investigated, that might help to focus future mission sensor decisions depending on their intended use cases. The addition of Machine Learning to the data fusion process greatly amplifies the utility and speed with which identification algorithms can be undertaken, and is an indicator of the direction much SAR and EO research will take in the future. This would also open the pathway for on-board algorithms for detection.

Acknowledgments

Thanks to SSTL for their assistance in providing the data for this report.

6 REFERENCES

1. SSTL confirms the successful launch of NovaSAR-1 and SSTL S1-4 satellites, 16/09/2018. https://www.sstl.co.uk/media-hub/latest-news/2018/sstl-confirms-the-successful-launch-of-novasar-1-a
2. SSTL S1-4: Launched 2018, 2018. https://www.sstl.co.uk/space-portfolio/launched-missions/2010-2020/sstl-s1-4-launched-2018
3. Bird, R. et al., "NovaSAR: Next Generation Developments", APSAR2015 Conference, September 2015.
4. WMO, Observing Systems Capability Analysis and Review Tool, Satellite: SSTL-S1-4, 2019. https://www.wmo-sat.info/oscar/satellites/view/766
5. Fingas, M. and C.E. Brown., "A Review of Oil Spill Remote Sensing", Sensors (Basel), 18(1): 91, January 2018. DOI: 10.3390/s18010091
6. Finch, I. and A. Antonacopoulos, "Identification of Airfield Runways in Synthetic Aperture Radar Images", Fourteenth International Conference on Pattern Recognition, 1998. DOI: 10.1109/ICPR.1998.712030
7. Bermudez, J. D. et al., "Synthesis of Multispectral Optical Images From SAR/Optical Multitemporal Data Using Conditional Generative Adversarial Networks", IEEE Geoscience and Remote Sensing Letters, Volume: 16 , Issue: 8 , August 2019, pp. 1220-1224. DOI: 10.1109/LGRS.2019.2894734
8. Bian, X., Y. Shao, W. Tian and C. Zhang, "Estimation of Shallow Water Depth Using HJ-1C S-band SAR Data", Journal of Navigation, pp. 113-126, 2016.
9. Sancho, F., F. Birrien, and A. Azevedo, "Co-ReSyF SAR-bathymetry application; algorithm testing and performance", Jornadas de Engenharia, pp. 41-44, 2018.
10. Boccia, V., A. Renga, G. Rufina, M. D'Errico, A. Moccia, C. Aragno, and S. Zoffoli, "Linear dispersion relation and depth sensitivity to swell parameters: Application to synthetic aperture radar imaging and bathymetry", Scientific World Journal, 2015.
11. Geyman, E., and A. Maloof, "A Simple Method for Extracting Water Depth From Multispectral Satellite Imagery in Regions of Variable Bottom Type", Earth and Space Science, pp. 527-537, 2019.
12. Lyzenga, D., "Passive remote sensing techniques for mapping water depth and bottom features", Applied Optics, 379, 1978.
13. Werner A., B. Holt and K. Zeng, "Oil spill detection by imaging radars: Challenges and pitfalls", IEEE International Geoscience and Remote Sensing Symposium (IGARSS), July 2017. DOI: 10.1109/IGARSS.2017.8127258
14. Hill, N., "Offshore Oil Spill Volume Estimation using SAR", Master's thesis, University of Surrey, 2018.